

Q-Space Undersampled Diffusional Kurtosis Imaging

A. Tabesh¹, J. H. Jensen¹, E. Fieremans¹, and J. A. Helpert^{1,2}

¹Radiology, New York University School of Medicine, New York, NY, United States, ²Medical Physics, Nathan Kline Institute, Orangeburg, NY, United States

Introduction

Diffusional kurtosis imaging (DKI) [1] is an extension of diffusion tensor imaging [2] which characterizes non-Gaussian water diffusion in biological tissues by estimating the kurtosis of the diffusion displacement distribution. A key advantage of DKI over other non-Gaussian techniques, such as diffusion spectrum imaging [3] and Q-ball imaging [4], is its shorter scan times, enabling its incorporation into routine clinical protocols. Nevertheless, further acceleration of the DKI acquisition can potentially facilitate its more widespread adoption. The DKI signal model is parameterized with six diffusion tensor (DT) and 15 kurtosis tensor (KT) parameters [1,5]. To determine these 21 parameters, the acquisition of at least 21 diffusion-weighted images (DWI's) is conventionally required, of which at least 15 DWI's must correspond to distinct q -space directions. Here, we assess the feasibility of reconstructing DKI parametric maps from q -space undersampled DKI scans. Extending our convex quadratic programming (QP)-based tensor estimation formulation [6], we present two constrained approaches that enable estimation of DKI maps from undersampled q -space data.

Theory

Constrained tensor estimation: The DT and KT are typically estimated via least-squares (LS) methods. In [6], we incorporated three sets of linear constraints into linear LS estimation to obtain a QP formulation of the tensor estimation problem. The constraints represent the prior knowledge about physically and biologically plausible estimates, and they were imposed on the minimum directional diffusivities, and on the minimum and maximum directional kurtoses. For undersampled DKI acquisitions, the formulation of [6] yields an underdetermined system of equations which, when consistent, has infinitely many solutions. Therefore, additional constraints are needed to ensure a unique solution. To address this drawback, we propose two types of constraints on the estimated tensors: a minimum (L_2) norm constraint (MNC); and, optionally, a sparsity constraint (SC). The SC requires the KT rotated into the frame of the DT eigenvectors (DTEV's) to have only six nonzero elements (justification given below). An additional shortcoming of applying the method of [6] to undersampled data is that the constraints on directional diffusivities and kurtoses along the acquisition gradient directions are insufficient, due to their limited number. This shortcoming can be alleviated by iteratively solving the QP problem, and augmenting the constraint set with additional constraints along the DTEV's obtained at the previous iteration. The modified QP formulation can thus be represented as

$$\text{Minimize } \|\mathbf{AX} - \mathbf{b}\|^2 \quad \text{such that } \mathbf{C}^{(i)}\mathbf{X} \leq \mathbf{d}^{(i)} \text{ and } \mathbf{A}^\perp\mathbf{X} = \mathbf{0},$$

where vector \mathbf{X} is a function of unknown DT and KT elements, matrix \mathbf{A} is a function of gradient directions and diffusion weightings, and vector \mathbf{b} is a function of diffusion signal intensities [6]. Matrix $\mathbf{C}^{(i)}$ and vector $\mathbf{d}^{(i)}$ represent the set of constraints on directional diffusivities and kurtoses at iteration i , and are generated by augmenting $\mathbf{C}^{(i-1)}$ and $\mathbf{d}^{(i-1)}$ to include additional constraints along the DTEV's obtained at iteration $i-1$, with $\mathbf{C}^{(0)}$ and $\mathbf{d}^{(0)}$ representing the constraints along the acquisition gradient directions. Matrix \mathbf{A}^\perp , whose rows form a basis for the null space of \mathbf{A} , is used to guarantee a unique solution satisfying the MNC. Note that \mathbf{X} has 12 or 21 elements, depending on whether or not the SC is imposed.

Sparsity constraint: The brain gray matter may be idealized as being isotropic with constant diffusivity and kurtosis along all directions. Due to this symmetry property, only six KT elements (W_{1111} , W_{2222} , W_{3333} , W_{1122} , W_{1133} , and W_{2233} ; with \mathbf{W} denoting the KT) will be nonzero. Parallel white matter bundles may be modeled using non-exchanging two-compartment models [7]. It is straightforward to show that for this model only the above six KT elements will be nonzero in the frame of DTEV's.

Methods

Reference and test DKI scans were performed on a healthy volunteer using a 3 T Siemens Tim Trio system with a 12-channel head coil. DWI's were acquired using a twice-refocused spin-echo sequence with parameters TR = 5500 ms, TE = 101 ms, matrix = 74×74 , FOV = 222×222 mm², 41 slices, slice thickness = 3 mm with no gap, no partial Fourier encoding, and parallel imaging with GRAPPA factor = 2. The reference scan consisted of DWI's acquired along $N = 30$ gradient directions with NEX = 2 for $b = 1000, 2000$ s/mm², and NEX = 11 for $b = 0$. Two test datasets were acquired with $N = 6$ and NEX = 1 for $b = 1000, 2000$ s/mm², and NEX = 1 for $b = 0$. The scan times for the reference and test datasets were 12 min 50 s and 88 s, respectively. Mean, axial, and radial kurtosis (MK, AK, and RK) maps were estimated for the test datasets using the proposed constrained methods and were compared to the maps obtained from the reference dataset using the QP method [6]. Prior to estimation, the DWI's were smoothed using a Gaussian kernel with a full width at half maximum of 3.375 mm.

Results

The statistics of the rotated KT elements in Figure 1 clearly show that the first six KT elements are much larger than the other elements, consistent with the prediction of the idealized models. The MK and RK maps obtained without the SC were smoother, but both maps had a tendency to underestimate the reference values, particularly for the MK (Figure 2). The AK maps (not shown) were particularly noisy. The root mean-square error (RMSE) values in Figure 3 indicate that the SC improved the MK estimates, but not the estimates of the AK and RK.

Discussion

We investigated the feasibility of obtaining parametric maps from q -space undersampled DKI acquisitions using extensions of the QP tensor estimation method presented in [6]. For highly undersampled DKI scans, using the SC resulted in more accurate MK maps, but less accurate AK and RK maps. The larger RMSE of the AK relative to its mean was expected, as calculating the AK does not involve averaging and therefore it is more affected by noise. Maps generated from the reference data with and without the SC were highly similar, perhaps indicating that the sparsity assumption holds for the majority of parenchyma voxels, an observation also supported by the statistics of the rotated KT elements in Figure 1. In conclusion, it is possible to obtain MK and RK maps from q -space undersampled DKI scans of usable quality and thereby substantially reduce the scan time.

References: 1. Jensen JH, et al. MRM 2005; 53:1432. 2. Basser PJ, et al. Biophys J 1994; 66:259. 3. Wedeen V, et al. ISMRM 2000; 8:82. 4. Tuch DS, et al. ISMRM 1999; 7:321. 5. Jensen JH, et al. NMR Biomed 2010; 23:698. 6. Tabesh A, et al. MRM 2011; DOI: 10.1002/mrm.22655. 7. Fieremans E, et al. ISMRM 2010; 18:1569.

Acknowledgments: Supported by NIH R01AG027852, NIH R01EB007656, and Litwin Foundation for Alzheimer's Research.

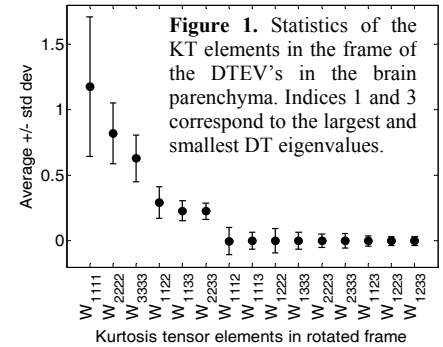


Figure 1. Statistics of the KT elements in the frame of the DTEV's in the brain parenchyma. Indices 1 and 3 correspond to the largest and smallest DT eigenvalues.

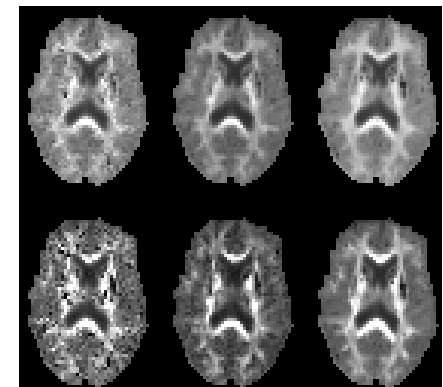


Figure 2. MK (top) and RK (bottom) maps obtained using q -space undersampling with (left) and without (center) the SC, together with fully sampled reference maps (right). The undersampled scans were acquired in 88 s, while the fully sampled scans took 8.84 times longer.

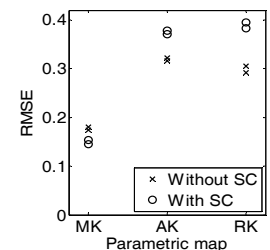


Figure 3. RMSE between the maps obtained from the two test datasets and the reference maps.